Supporting Information

Facile preparation of methanol catalyst with ultra-high voltage efficiency and super-durability: Pt pollution introduction by composite electrodeposition

Hao Lei, [a,c] *Mangwei Cui,*[a,c] *Wenzheng Li* [a,c] *and Yan Huang**[a,b,c]

[a]Sauvage Laboratory for Smart Materials, School of Materials Science and Engineering, Harbin Institute of Technology (Shenzhen), Shenzhen 518055, China.

[b]State Key Laboratory of Advanced Welding and Joining, Harbin Institute of Technology, Harbin 150001, China.

[c]Shenzhen Key Laboratory of Flexible Printed Electronics Technology, Harbin Institute of Technology (Shenzhen), Shenzhen 518055, China.

*e-mail: yanhuanglib@hit.edu.cn

Experimental Section

Chemicals and reagents

Ethylene glycol (EG, 99%), cobalt chloride hexahydrate ($CoCl_2 \cdot 6H_2O$, 98%), potassium hydroxide (KOH, 98%), tin chloride ($SnCl_4$, 98%), Choline chloride (ChCl, 98%) and nickel plate (purity > 99.99%) were purchased from Sinopharm Chemical Reagent Co., LTD. Nafion solution (5 wt.%) and commercial Pt/C (20 wt.% Pt) catalysts were obtained from Sigma-Aldrich (St. Louis, MO, USA). Milli-Q deionized water (18.2 $M\Omega$ cm^{-1}) was used throughout the experiment. Analytical grade reagents were used without further purification. EG and ChCl were stirred at 353 K for 2 h at a molar ratio of 2:1 to prepare typical deep eutectic solvent ethaline.

Synthesis of CoSn-Pt, Co-Pt, Sn-Pt, CoSn, Co and Sn

First, appropriate amounts of $CoCl_2$ and $SnCl_4$ were added to the ethaline solvent (40 mL) so that their concentrations were 100 mM and 50 mM, respectively. After being heated to 353 K and stirred well, a blue transparent solution was obtained. The electrolyte used for composite electrodeposition Pre-CoSn-Pt was obtained by preparing Pt nanoparticles in ethaline solution containing 100 mM $CoCl_2$ and 50 mM $SnCl_4$ through potentiostatic deposition (-0.8 V vs. Ag, 4000 s, 353K). This process was completed in the three electrode system controlled by CHI workstation (CHI 760E). Nickel plate (exposure area=0.25 cm^2), Pt plate (exposure area=2 cm^2) and Ag wire (Φ= 1 mm) were used as working electrode, counter and reference electrode respectively. The solution gradually changed from blue to opaque dark blue-black during the generation of Pt particles (According to the ICP-MS test results, the concentration of Pt atoms in the composite deposition electrolyte is 1.3 mM). The method for preparing Pre-Co-Pt and Pre-Sn-Pt composite electrodeposition electrolyte is similar to that for preparing Pre-CoSn-Pt composite electrodeposition electrolyte. The difference is that when preparing composite electrodeposition electrolyte, ethaline solution containing 100 mM $CoCl_2$ and ethaline solution containing 50 mM $SnCl_4$ are used to replace the ethaline solution containing 100 mM $CoCl_2$ and 50 mM $SnCl_4$ respectively.

The composite electrodeposition process was carried out in the same three-electrode system as in the previous step. The composite electrodeposition process parameters are temperature

353 K, voltage -0.65 V vs. Ag, time 400 s. Before deposition, the nickel plate was ultrasonically cleaned in ethanol and 2 M HCl for 5 min, then in deionized water and dried at room temperature. The deposited sample was washed several times with ethanol and deionized water. In addition to replacing the electrolyte with ethaline solution containing 100 mM $CoCl_2$, ethaline solution containing 50 mM $SnCl_4$ and ethaline solution containing 100 mM $CoCl_2$ and 50 mM $SnCl_4$ as the electrolyte and using a graphite plate as the counter electrode, the preparation process of Pre-Co, Pre-Sn and Pre-CoSn is the same as that of Pre-CoSn-Pt.

CoSn-Pt, Co-Pt, Sn-Pt, CoSn, Co and Sn were obtained by multiple cyclic voltammetry (CV) tests in standard three-electrode cell by placing Pre-CoSn-Pt, Pre-CoSn Pre-Co and Pre-Sn in 1 M KOH solution, respectively. Carbon rod and Ag/AgCl (3 M KCl) were used as counter electrode and reference electrode. The CV scanning range was 0.174 V to 1.324 V vs. RHE, the scanning speed was 50 mV s^{-1}, and the scanning temperature was 298 K.

Synthesis of S-C_3N_4/CNT

Multi-walled CNTs (50 mg), thiourea (25 mg), trimesic acid (25 mg) and dicyandiamide (25 mg) were added to 10 mL of ethanol, stirred for 3 h, and then dried under vacuum. The dried powder was annealed at 800 °C for 3 h at a heating rate of 5 °C min^{-1} in an argon atmosphere. This product is denoted as S-C_3N_4/CNT.

Synthesis of sodium polyacrylate (PANa) hydrogel electrolyte

The synthesis method of PANA hydrogel electrolyte refers to the previous work of our group[1]. First, The AA solution (prepared by adding acrylic monomer (AA, 48 g) to deionized water (54 g) in ice bath) was gradually infused with the sodium hydroxide solution (prepared by adding sodium hydroxide (26.7 g) to deionized water (18 g) at room temperature). After full neutralization, a sodium acrylate solution was obtained. Then, ammonium persulfate (APS, 0.78 g) was added to initiate free-radical polymerization proceeding steadily in an oven at 60 °C for 20 h. Finally, the prepared PANa hydrogel was stripped and fully dried in an oven at 80 °C, and then soaked in a mixed solution (500 mL) of potassium hydroxide (5 mol/L) and methanol (1 mol/L) for one week to achieve concentration balance. The volume of hydrogel used in the flexible direct methanol fuel cell is 5 cm^3 (containing 0.16 g methanol).

Fabrication of the flexible DMFCs

A PANa hydrogel diaphragm was sandwiched between two carbon fiber cloths evenly coated with catalyst, and then a simple sandwich structure was formed by using thin wires at both ends. In this structure, air can directly diffuse to the surface of the S-C_3N_4/CNT catalyst (the matrix was an exposed high-permeable carbon fiber cloth) and be reduced. On the anode side, methanol in the gel electrolyte underwent methanol oxidation reaction catalyzed by CoSn-Pt and Pt/C, respectively. PANa hydrogel electrolyte was responsible for ion transport during the reaction. The flexible DMFCs we created with a simple structure and fabrication process are easy to operate and do not require other conditions.

Characterization

The elemental composition and microstructure of the samples were revealed by a Tecnai G2 F30J field-emission TEM equipped with EDX. The morphology of the prepared samples was characterized by field emission scanning electron microscope (FE-SEM, NOVA NanoSEM 450). X-ray photoelectron spectra (XPS) were conducted using a Thermo Scientific ESCALAB 250Xi instrument equipped with an Al X-ray excitation source. Raman scattering measurements were performed with a multichannel modular triple Raman system (Renishaw Co.) with confocal microscopy at room temperature using the 514 nm laser. The *in-situ* ATR-IR measurements were conducted using a Nicolet iS50 FT-IR spectrometer equipped with a MCT detector cooled by liquid nitrogen, at a spectral resolution of 4 cm^{-1} and with p-polarized IR radiation. The rate of dynamic potential scanning is 10 mV/s, which is controlled by the electrochemical workstation (CHI 760E). The inductively coupled plasma mass spectrometry (ICP-MS, PerkinElmer ELAN DRC-e,) is used to detect the content of each element in the samples. CO temperature-programmed desorption (CO-TPD) was performed on FINESORB-3010 equipped with a thermal conductivity detector (TCD). ~ 5 mg catalysts were put in a U-shape quartz tube and heated to 300 °C in a Ar flow (40 mL/min) with a heating rate of 10 °C/min, and then cooled down to room temperature in the same Ar flow. Afterwards, the sample was exposed to CO for 10 min. Finally, the sample was flushed with Ar (40 mL/min) for 15 min at room temperature and then heated to 600 °C with a rate of 10 $°C\cdot min^{-1}$ in the same Ar flow. The temperature and current of TCD were 60 °C and 90 mA, respectively.

Electrochemical measurements

All electrochemical tests are conducted by Shanghai Chenhua 760E electrochemical workstation. The test system is a traditional three-electrode system, with the prepared sample as the working electrode, the Pt column electrode as the counter electrode, and the Ag/AgCl (3.0 M KCl) electrode as the reference electrode. Cyclic voltammetry was carried out in 1.0 M KOH + 0.5 M CH_3OH solution at 298 K, and the scanning range was 0.174 V to 1.324 V vs. RHE at a scan rate of 50 mV s^{-1}. The electrochemical impedance spectroscopy (EIS) test is measured at a given overpotential in the frequency range of 5 mHz to 100 kHz, with an AC voltage amplitude of 5 mV. All measured potentials were converted to the RHE using $E_{RHE} = E_{Ag/AgCl} + 0.198 + 0.059 \times pH$.

Commercial Pt/C electrode was prepared by two steps. In the first step, Pt/C (4 mg) and Nafion (30 uL, 5 wt.%) were dispersed in 0.47 mL isopropyl alcohol solution and ultrasonic treatment was conducted for 10 min to obtain homogeneous catalyst ink. Then, 12 μL of catalyst ink was loaded on the nickel plate (working area: 0.5 cm^2). The mass load of Pt is approximately 38.4 μg cm^2.

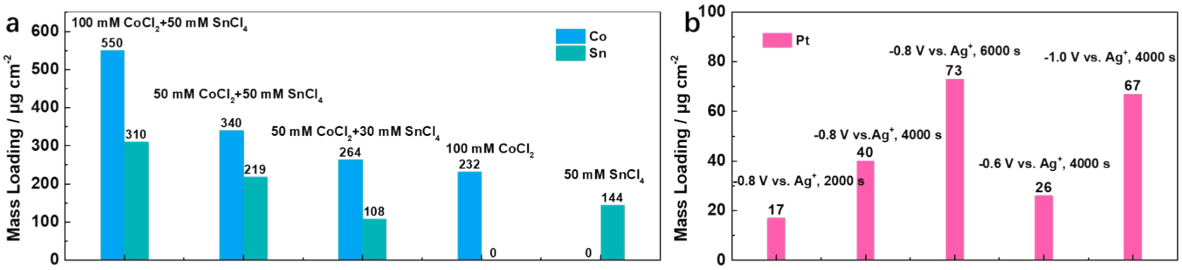

Fig. S1 Mass loading change diagram of elements in the catalyst when changing the concentration of metal salt precursor (a), and changing Pt corrosion conditions (b).

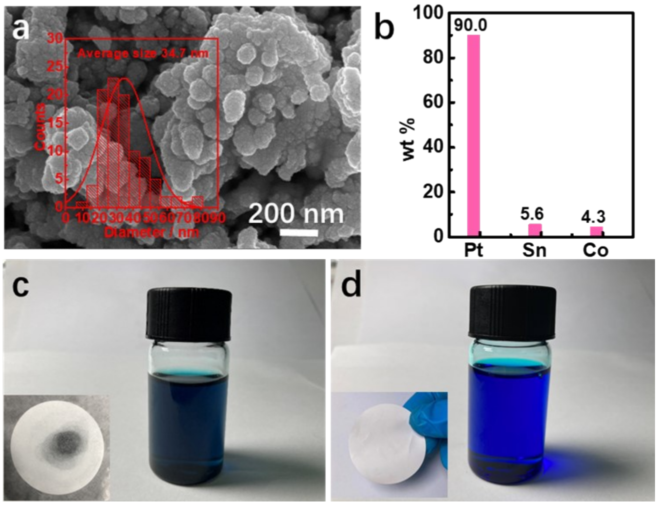

Fig. S2 (a) SEM image of Pt particles in suspension. The inset indicates the particle size histogram. (b) Mass percentage of individual element in Pt particles (a small amount of Co and Sn may originate from the exfoliation of a small amount of coating on the cathode). (c) Electrolyte used in composite electrodeposition (ethaline with 100 mM $CoCl_2$ + 50 mM $SnCl_4$ + Pt particles). The inset is a photograph of particles obtained by suction filtration of the suspension. (d) Electrolyte used in electrodeposition (ethaline with 100 mM $CoCl_2$ + 50 mM $SnCl_4$). The inset is a photograph of the filter paper obtained by suction filtration of the electrolyte.

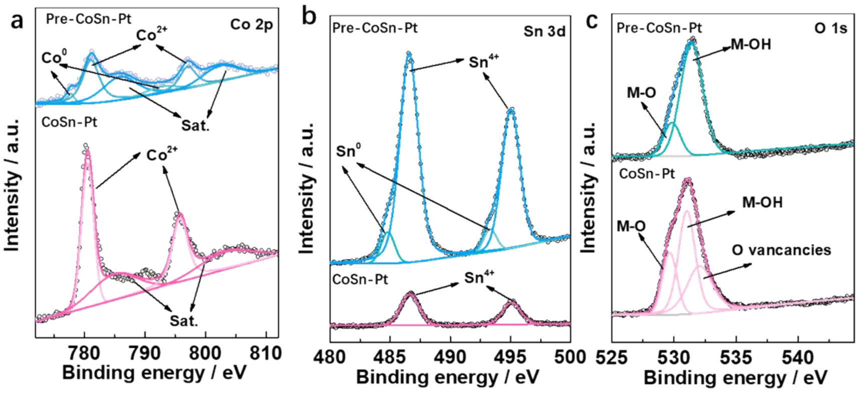

Fig. S3 XPS spectra of Pre-CoSn-Pt and CoSn-Pt: (a) Co 2p, (b) Sn 3d, (c) O 1s.

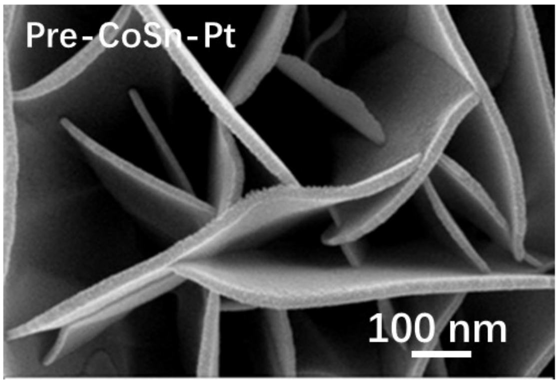

Fig. S4 SEM image of Pre-CoSn-Pt.

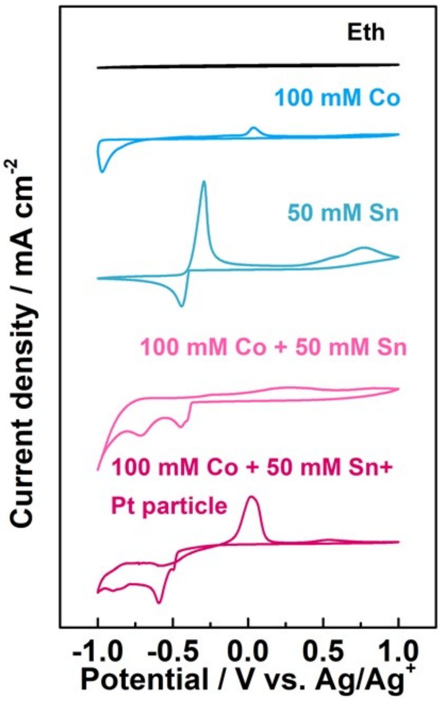

Fig. S5 CVs of ethaline, ethaline with 100 mM $CoCl_2$, ethaline with 50 mM $SnCl_4$, ethaline with 100 mM $CoCl_2$ + 50 mM $SnCl_4$ and ethaline with 100 mM $CoCl_2$ + 50 mM $SnCl_4$ + Pt particles recorded on a Ni electrode under a scan rate of 0.01 V s^{-1}.

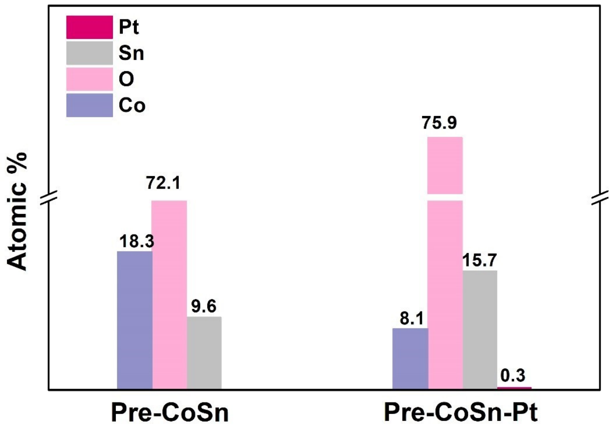

Fig. S6 Atomic percentage of individual element on the surface of Pre-CoSn and Pre-CoSn-Pt (Element content data from XPS).

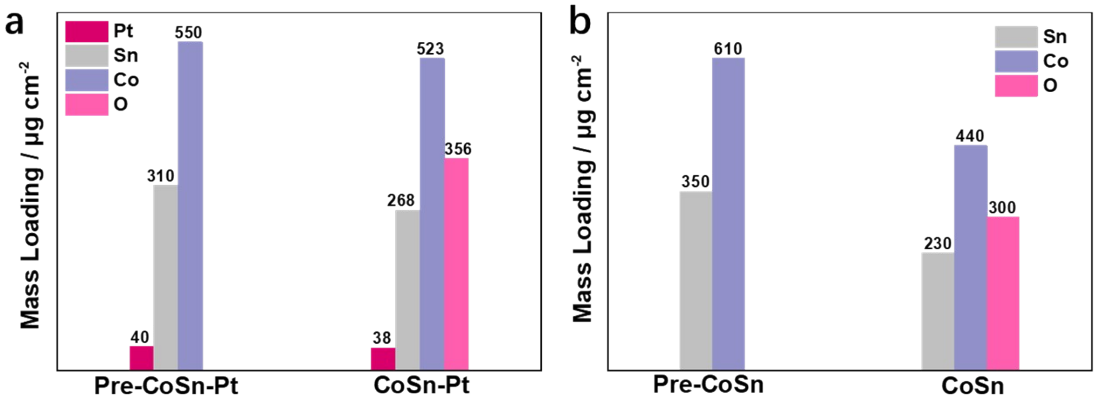

Fig. S7 (a) The mass loading of each element in Pre-CoSn-Pt and CoSn-Pt. (b) The mass loading of each element in Pre-CoSn and CoSn. The data for Pt, Co and Sn are from ICP-MS, and data for O is calculated from SnO_2 and $Co(OH)_2$.

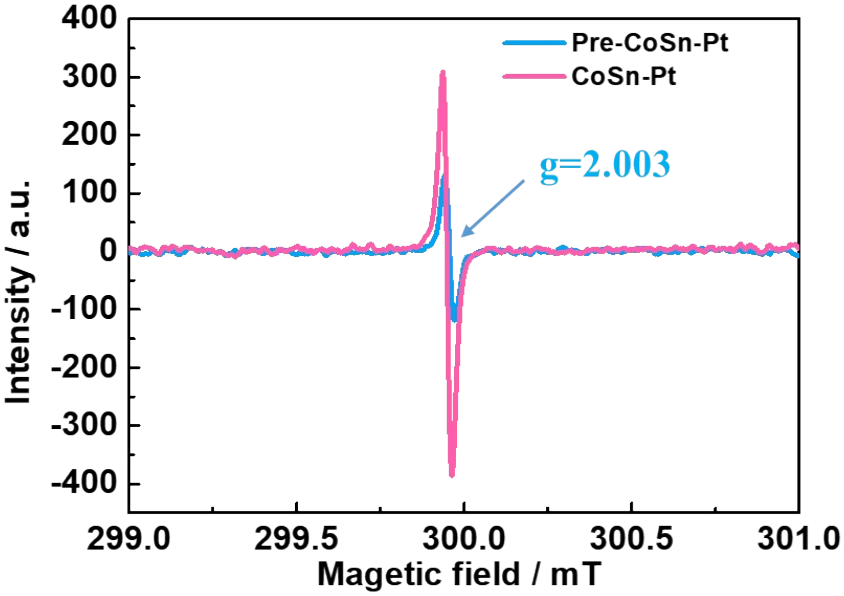

Fig. S8 EPR spectra of Pre-CoSn-Pt and CoSn-Pt.

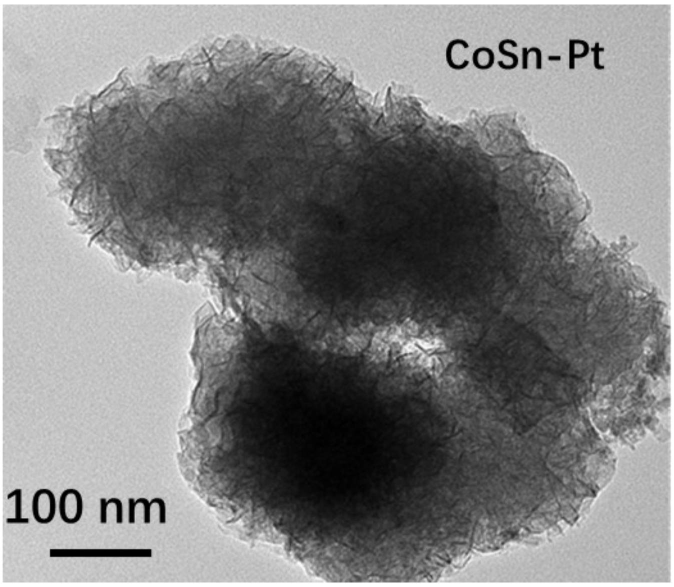

Fig. S9 TEM image of CoSn-Pt.

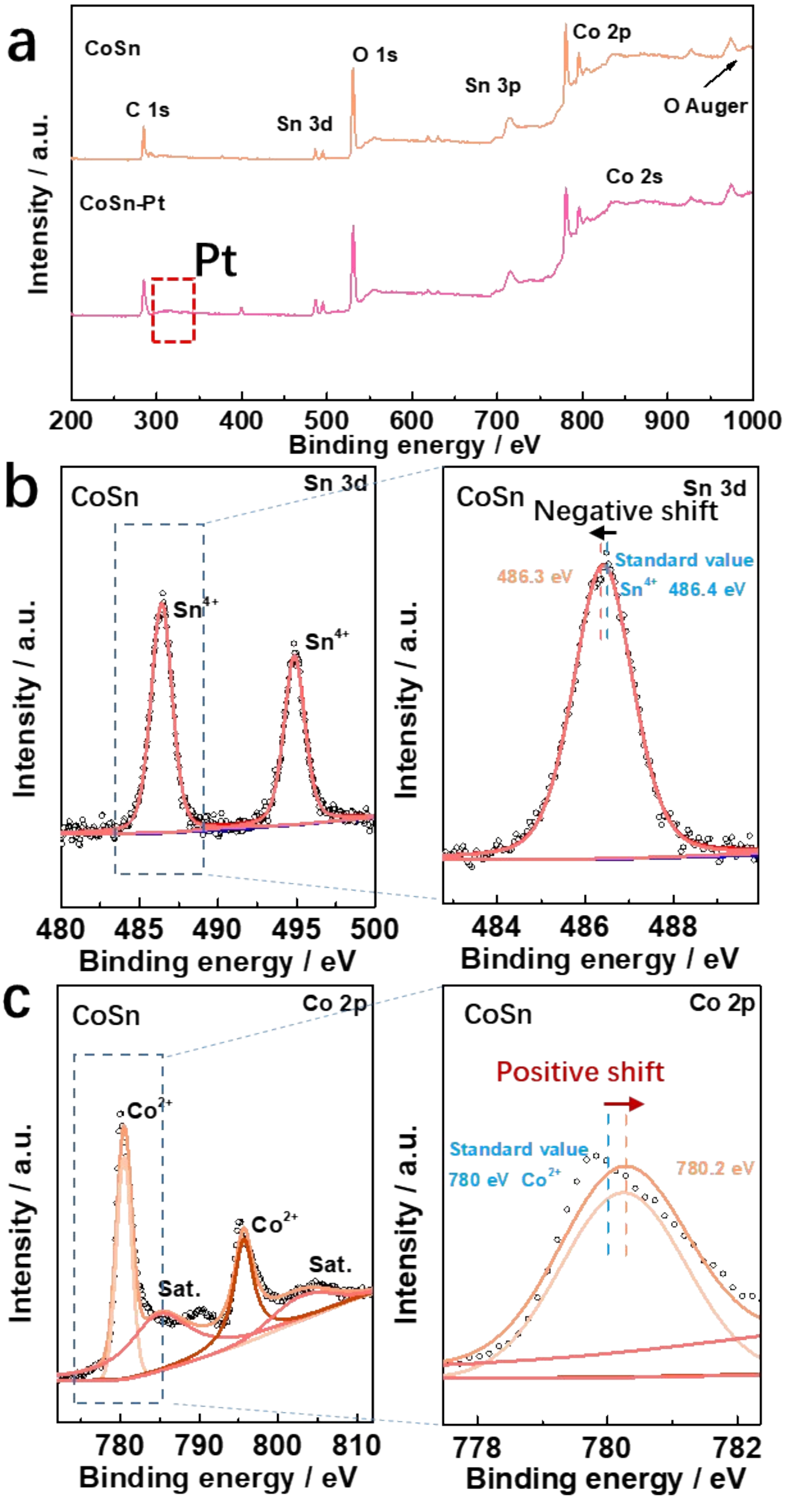

Fig. S10 (a) Full XPS survey of CoSn and CoSn-Pt. High-resolution XPS spectra of CoSn in (b) Sn 3d, (c) Co 2p regions.

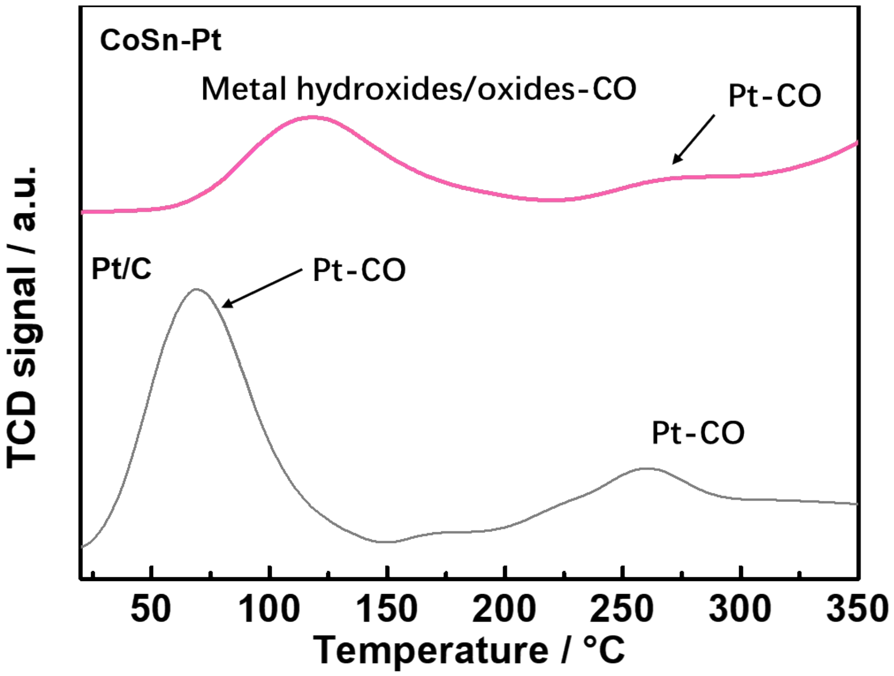

Fig. S11 CO-TPD profiles of Pt/C and CoSn-Pt.

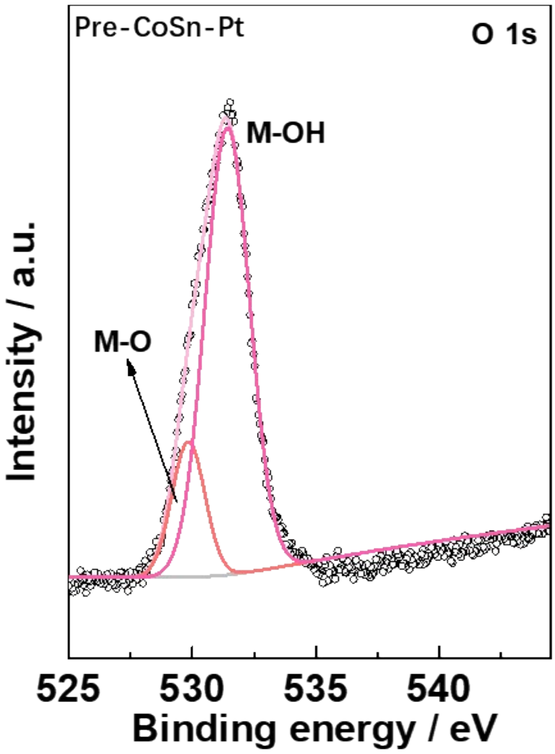

Fig. S12 High resolution XPS spectra of O 1s of Pre-CoSn-Pt.

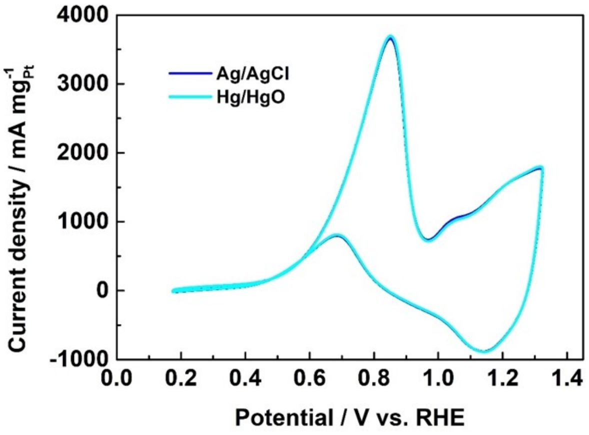

Fig. S13 CV curves of CoSn-Pt when Ag/AgCl and Hg/HgO are used as reference electrodes in N_2-saturated 1 M KOH+ 0.5 M CH_3OH solution, respectively.

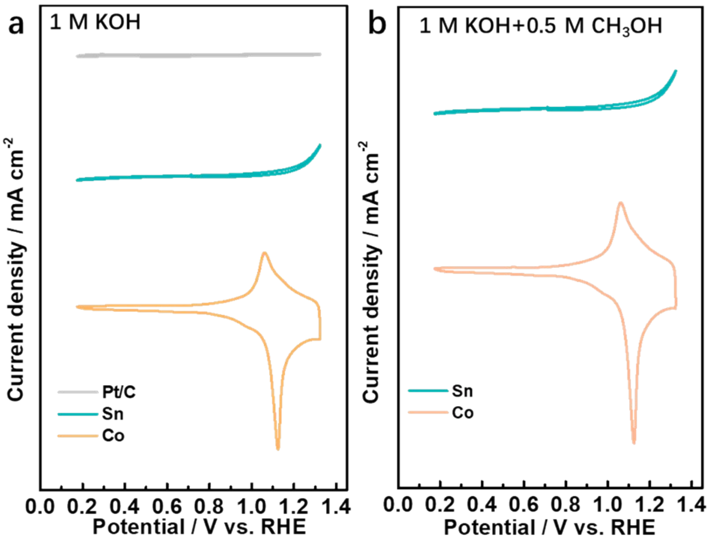

Fig. S14 CV curves of Sn, Co and Pt/C at a scan rate of 50 mV s^{-1} in N_2-saturated (a) 1 M KOH solution and (b) 1 M KOH + 0.5 M CH_3OH solution.

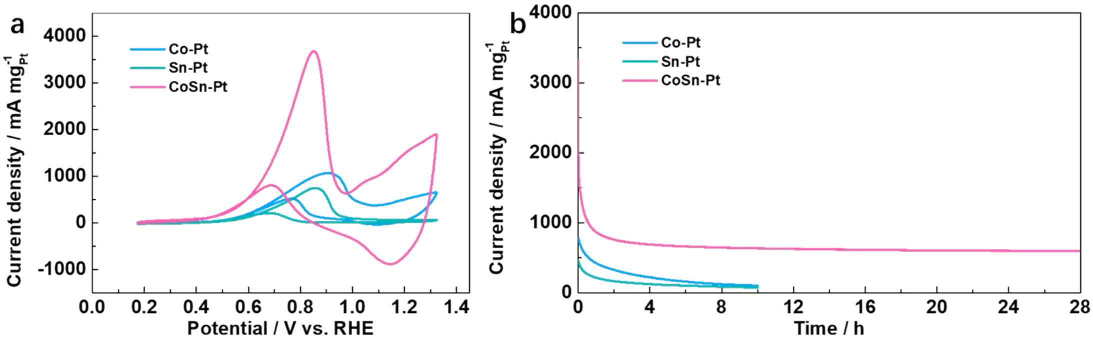

Fig. S15 (a) CV curves of Co-Pt, Sn-Pt and CoSn-Pt at a scan rate of 50 mV s^{-1} in N_2-saturated 1 M KOH + 0.5 M CH_3OH solution. (b) Chronoamperometry curves of three MOR catalysts recorded at 0.8 V vs. RHE.

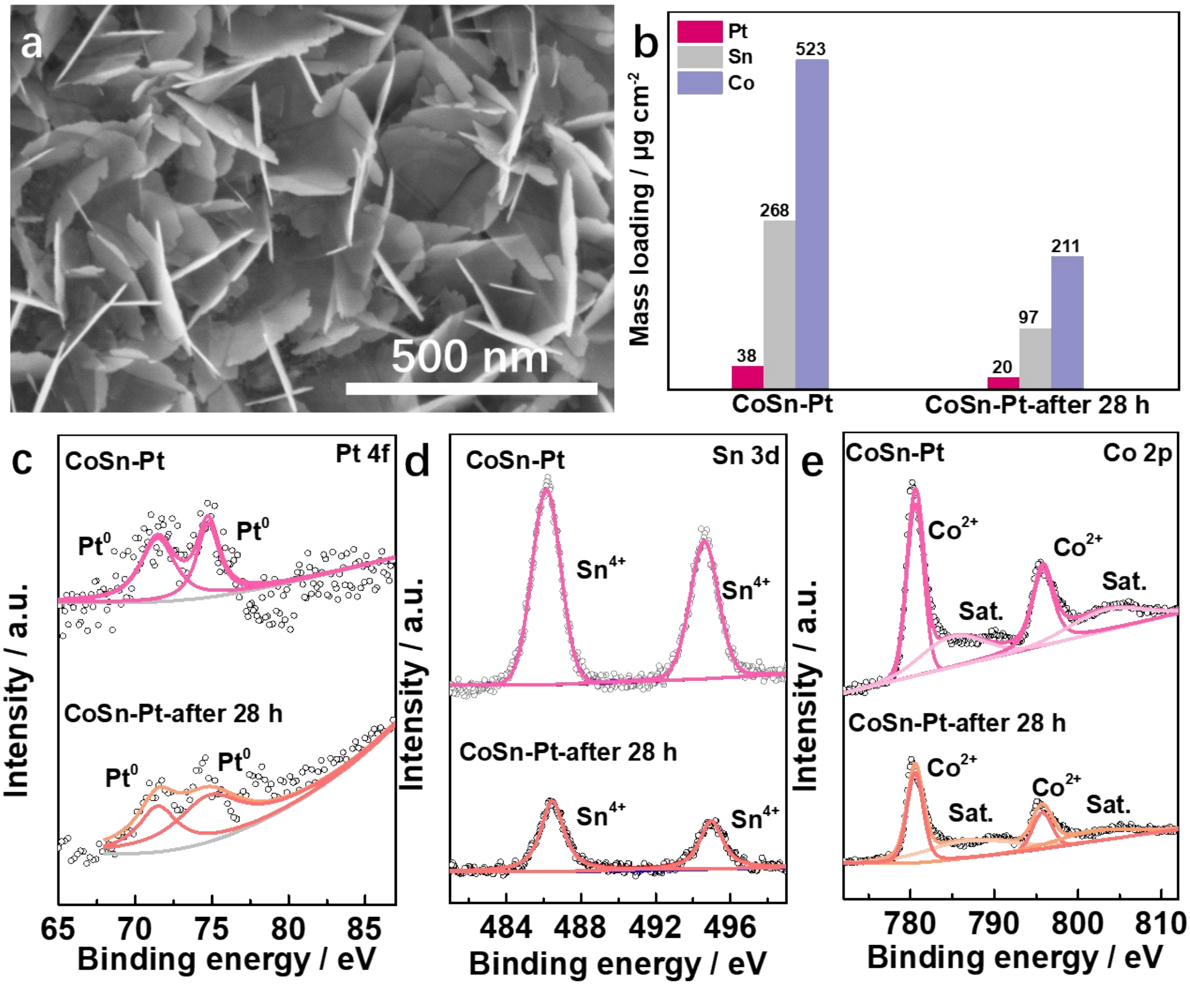

Fig. S16 (a) SEM image of CoSn-Pt-after 28 h; (b) Mass loading of individual element in CoSn-Pt and CoSn-Pt-after 28 h; XPS spectra of CoSn-Pt and CoSn-Pt-after 28 h: (c) Pt 4f, (d) Sn 3d, (e) Co 2p.

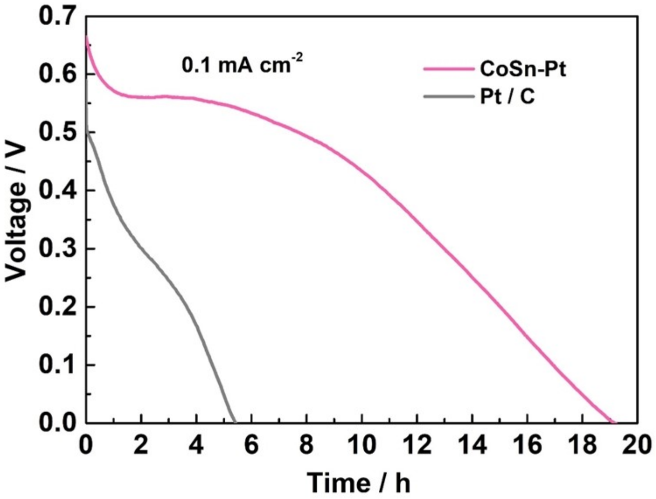

Fig. S17 Discharge curves of flexible direct methanol fuel cells based on Pt/C and CoSn-Pt anodes at 0.1 mA cm^{-2}.

Table S1. Comparison of CoSn-Pt with other electrocatalysts for MOR.

Electrode	**Medium**	**Mass Activity / mA mg^{-1}$_{\mathrm{metal}}$**	**Stability (CA test)**			**Ref.**
			i_o / mA mg^{-1}$_{\mathrm{metal}}$	Hold time / h	i_t / mA mg^{-1}$_{\mathrm{metal}}$	
single Pt atoms on Ru	0.1 M $HClO_4$ + 1.0 M CH_3OH	1580 mA·mg^{-1}$_{\mathrm{Pt}}$	1100	4	220	2
A-PNTs	0.5 m H_2SO_4 + 1.0 M CH_3OH	2560 mA·mg^{-1}$_{\mathrm{Pt}}$	115	1	10	3
Pd-PdO PNTs-260	1.0 M KOH + 1.0 M CH_3OH	1111.3 mA·mg^{-1}$_{\mathrm{Pd}}$	52	2.78	12	4
Au_3Ag nanoframes	0.5 M KOH + 2 M CH_3OH	950 mA·mg^{-1}$_{\mathrm{Au}}$	950	20	3.2	5
Pd-CeO_2/NMCS	1 M KOH + 1 M CH_3OH	1500 mA·mg^{-1}$_{\mathrm{Pd}}$	292	1	109.4	6
PtRu NWs /C	0.1 M $HClO_4$ + 0.5 M CH_3OH	820 mA·mg^{-1}$_{\mathrm{Pt}}$	810	1.11	200	7
Pt−Co nanoframes	1 M KOH + 1 M CH_3OH	4280 mA·mg^{-1}$_{\mathrm{Pt}}$	1010	0.5	330	8
PtZn/MWNT	0.1M KOH + 0.5 M CH_3OH	~550 mA·mg^{-1}$_{\mathrm{Pt}}$	750	0.25	110	9
SANi-PtNWs	1 M KOH + 1 M CH_3OH	7930 mA·mg^{-1}$_{\mathrm{Pt}}$	1000	1	760	10
Pt-SnO_2/rGO	1 M $HClO_4$ +1 M CH3OH	1310 mA·mg^{-1}$_{\mathrm{Pt}}$	572	1	301	11
22% YO_x/MoO_x–Pt	0.1 M $HClO_4$ + 0.5 M CH_3OH	2100 mA·mg^{-1}$_{\mathrm{Pt}}$	350	0.83	120	12
Pt/Ni$(OH)_2$/rGO-4	1 M KOH + 1 M CH_3OH	1236 mA·mg^{-1}$_{\mathrm{Pt}}$	610	0.83	480	13
Pt_5Nd/C	1 M KOH + 1 M CH_3OH	4520 mA·mg^{-1}$_{\mathrm{Pt}}$	570	1.39	60	14
PtPdRuTe Nanotubes	0.5 M H_2SO_4 + 1.0 M CH_3OH	1261.5 mA·mg^{-1}$_{\mathrm{Pt}}$	280	1	30	15
Highly crystalline PtCu nanotubes	0.5 M H_2SO_4 + 1.0 M CH_3OH	2252 mA·mg^{-1}$_{\mathrm{Pt}}$	530	0.83	70	16
single Pt atoms on Ru	0.1 M $HClO_4$ + 1.0 M CH_3OH	1580 mA·mg^{-1}$_{\mathrm{Pt}}$	810	4	210	17
CoSn-Pt	1 M KOH + 0.5 M CH_3OH	3680 mA·mg^{-1}$_{\mathrm{Pt}}$	2800	28	610	This Work

References:

[1] J. Wang, Z. Pei, J. Liu, M. Hu, Y. Feng, P. Wang, H. Wang, N. Nie, Y. Wang, C. Zhi and Y. Huang, *Nano Energy,* 2019, **65**, 104052.

[2] M. Qiao, H. Wu, F. Y. Meng, Z. Zhuang and J. X. Wang, *Small,* 2022, **18**, 2106643.

[3] F. Xu, S. Cai, B. Lin, L. Yang, H. Le and S. Mu, *Small,* 2022, **18**, 2107387.

[4] T. J. Wang, F. M. Li, H. Huang, S. W. Yin, P. Chen, P. J. Jin and Y. Chen, *Adv. Funct. Mater.* 2020, **30**, 2000534.

[5] L. Xiong, Z. Sun, X. Zhang, L. Zhao, P. Huang, X. Chen, H. Jin, H. Sun, Y. Lian, Z. Deng, M. H. Rummerli, W. Yin, D. Zhang, S. Wang and Y. Peng, *Nat. Commun.,* 2019, **10**, 3782.

[6] Q. Tan, C. Shu, J. Abbott, Q. Zhao, L. Liu, T. Qu, Y. Chen, H. Zhu, Y. Liu and G. Wu, *ACS Catal.,* 2019, **9**, 6362-6371.

[7] L. Huang, X. Zhang, Q. Wang, Y. Han, Y. Fang and S. Dong, *J. Am. Chem. Soc.,* 2018, **140**, 1142-1147.

[8] S. Chen, M. Li, M. Gao, J. Jin, M. A. van Spronsen, M. B. Salmeron and P. Yang, *Nano Lett.,* 2020, **20**, 1974-1979.

[9] Z. Qi, C. Xiao, C. Liu, T. W. Goh, L. Zhou, R. Maligal-Ganesh, Y. Pei, X. Li, L. A. Curtiss and W. Huang, *J. Am. Chem. Soc.,* 2017, **139**, 4762-4768.

[10] M. Li, K. Duanmu, C. Wan, T. Cheng, L. Zhang, S. Dai, W. Chen, Z. Zhao, P. Li, H. Fei, Y. Zhu, R. Yu, J. Luo, K. Zang, Z. Lin, M. Ding, J. Huang, H. Sun, J. Guo, X. Pan, W. A. Goddard, P. Sautet, Y. Huang and X. Duan, *Nat. Catal.,* 2019, **2**, 495-503.

[11] Y.-W. Zhou, Y.-F. Chen, K. Jiang, Z. Liu, Z.-J. Mao, W.-Y. Zhang, W.-F. Lin and W.-B. Cai, *Appl. Catal. B: Environ.,* 2021, **280**, 119393.

[12] M. Li, Z. Zhao, W. Zhang, M. Luo, L. Tao, Y. Sun, Z. Xia, Y. Chao, K. Yin, Q. Zhang and L. Gu, W. *Adv. Mater.,* 2021, **33**, 2103762.

[13] W. Huang, H. Wang, J. Zhou, J. Wang, P. N. Duchesne, D. Muir, P. Zhang, N. Han, F. Zhao, M. Zeng, J. Zhong, C. Jin, Y. Li, S. T. Lee and H. Dai, *Nat. Commun.,* 2015, **6**, 10035.

[14] S. Zhang, Z. C. Zeng, Q. Q. Li, B. L. Huang, X. Y. Zhang, Y. P. Du and C. H. Yan, *Energy Environ. Sci.,* 2021, **14**, 5911-5918.

[15] S. Y. Ma, H. H. Li, B. C. Hu, X. Cheng, Q. Q. Fu and S. H. Yu, *J. Am. Chem. Soc.* 2017,

139, 5890-5895.

[16] H.-H. Li, Q.-Q. Fu, L. Xu, S.-Y. Ma, Y.-R. Zheng, X.-J. Liu and S.-H. Yu, *Energy Environ. Sci.,* 2017, **10**, 1751-1756.

[17] A. R. Poerwoprajitno, L. Gloag, J. Watt, S. Cheong, X. Tan, H. Lei, H. A. Tahini, A. Henson, B. Subhash, N. M. Bedford, B. K. Miller, P. B. O'Mara, T. M. Benedetti, D. L. Huber, W. Zhang, S. C. Smith, J. J. Gooding, W. Schuhmann and R. D. Tilley, *Nat. Catal.,* 2022, **5**, 231-237.